Novel pathogenic variants in filamin C identified in pediatric restrictive cardiomyopathy

Jeffrey Schubert[1,2], Muhammad Tariq[3], Gabrielle Geddes[4], Steven Kindel[4], Erin M. Miller[5], and Stephanie M. Ware[2].

[1] Department of Molecular Genetics, Microbiology, and Biochemistry, University of Cincinnati College of Medicine, Cincinnati, OH; [2] Departments of Pediatrics and Medical and Molecular Genetics, Indiana University School of Medicine, Indianapolis, IN; [3] Faculty of Applied Medical Science, University of Tabuk, Tabuk, Kingdom of Saudi Arabia; [4] Department of Pediatrics, Medical College of Wisconsin, Milwaukee, WI; [5] Cincinnati Children's Hospital Medical Center, Cincinnati, OH.

Correspondence:

Stephanie M. Ware, MD, PhD

Department of Pediatrics

Indiana University School of Medicine

1044 W. Walnut Street

Indianapolis, IN 46202

Telephone: 317 274-8939

Email: stware@iu.edu

_____

Abstract

Restrictive cardiomyopathy (RCM) is a rare and distinct form of cardiomyopathy characterized by normal ventricular chamber dimensions, normal myocardial wall thickness, and preserved systolic function. The abnormal myocardium, however, demonstrates impaired relaxation. To date, dominant variants causing RCM have been reported in a small number of sarcomeric or cytoskeletal genes, but the genetic causes in a majority of cases remain unexplained especially in early childhood. Here, we describe two RCM families with childhood onset: one in a large family with a history of autosomal dominant RCM and the other a family with affected monozygotic, dichorionic/diamniotic twins. Exome sequencing found a pathogenic filamin C (*FLNC*) variant in each: p.Pro2298Leu which segregates with disease in the large autosomal dominant RCM family, and p.Tyr2563Cys in both affected twins. *In vitro* expression of both mutant proteins yielded aggregates of FLNC containing actin in C2C12 myoblast cells. Recently, a number of variants in *FLNC* have been described that cause hypertrophic, dilated, and restrictive cardiomyopathies. Our data presented here provide further evidence for the role of *FLNC* in pediatric RCM, and suggest the need to include *FLNC* in genetic testing of cardiomyopathy patients including those with early ages of onset.

Key Words: variant interpretation, exome sequencing, heart failure, protein aggregation, heart transplant

Introduction

Cardiomyopathy (CM), a disease of heart muscle causing systolic and/or diastolic dysfunction, is a common cause of cardiac failure in children (Wilkinson, Westphal, Ross, Dauphin, & Lipshultz, 2015). Phenotypes include dilated (DCM), hypertrophic (HCM), restrictive (RCM), and arrhythmogenic forms (AVC), as well as left ventricular noncompaction (LVNC). RCM, the rarest of the cardiomyopathies, is defined as restrictive ventricular physiology in the presence of normal or reduced diastolic volumes, normal or reduced systolic volumes, and normal ventricular wall thickness (Vatta & Towbin, 2011). RCM accounts for up to 5% of cardiomyopathies in children, with the majority having no specific cause identified. The prognosis in children with RCM is poor—nearly 50% of patients die or undergo transplant within 3 years of diagnosis (Russo, 2005; Webber et al., 2012). Familial RCM is reported in 30% of all cases and both autosomal recessive and autosomal dominant inheritance have been described (Denfield & Webber, 2010). In some families with autosomal dominant cardiomyopathy, both HCM and RCM have been identified, suggested shared genetic causes (Kaski, Biagini, Lorenzini, Rapezzi, & Elliott, 2014). To date more than 100 genes have been implicated in various forms of CM (Tariq & Ware, 2014; Ware, 2015; Ware, 2017). These genes are involved in sarcomere, cytoskeleton, desmosome or mitochondria organization, metabolic processes, and other additional cellular functions (Harvey & Leinwand, 2011).

Despite progress in identifying various genetic causes for cardiomyopathies, little is known about the genetic etiology of RCM. To date, dominant pathogenic variants causing RCM have been reported in *DES*, *ACTC1, TNNI3, TNNT2, TPM1, MYL3, MYL, MYPN, TTN, BAG3, FLNC, TTR* and *MYH7,* but the majority of cases are considered idiopathic (Towbin, 2014). However, recent studies of idiopathic RCM cohorts tested using panels of 100-200 cardiomyopathy-related genes show some success in identifying additional likely pathogenic

variants in genes including: *DES, LAMP2, LMNA, BAG3, JUP, TTN,* and others, with 50-60% of patients having an identified potentially pathogenic variant (Gallego-Delgado et al., 2016; Kostareva et al., 2016). Although previous reports indicate yields of clinical genetic testing around 20% for RCM (Ackerman et al., 2011), data are limited. Identification of further genetic causes for RCM will be the first step for understanding the disease mechanisms, which may eventually lead to gene-specific diagnosis and potential therapy.

Filamins are a group of large proteins important for structural integrity of cells that act by crosslinking actin filaments and anchoring membrane proteins to the cytoskeleton. Variants in *FLNC* have not only been reported in RCM patients but also in other cardiomyopathies and skeletal muscle diseases (Brodehl et al. 2016 and Valdés-Mas et al., 2014; Vorgerd et al., 2005). In this study, we investigated two families with early onset RCM, identified *FLNC* variants using an exome sequencing (ES) approach, and performed *in vitro* functional analyses. Using these approaches, we sought to expand the current spectrum of genetic variants associated with familial RCM.

Methods

Ascertainment of familial RCM and ethical considerations

Patients underwent clinical evaluation by a pediatric geneticist and pediatric cardiologist at Cincinnati Children's Hospital Medical Center (CCHMC) or Children's Hospital of Wisconsin. Patients and family members enrolled in a research study approved by the Institutional Review Boards (IRB) at CCHMC or Indiana University. Written informed consent for participation in this study, as well as publication of clinical data of the affected individuals was obtained from the families. All the methods applied in this study conformed to the Declaration of Helsinki (1964) of the World Medical Association concerning human material/data and experimentation. Genomic DNA of 6 individuals from Family 1 (Fig. 1A)

or 5 individuals from Family 2 (Fig. 2A) was extracted from whole peripheral blood leukocytes following a standard DNA extraction protocol (Promega, Madison, WI).

Exome sequencing

For Family 1, ES was performed on a research basis. Genomic DNA (2μg) from proband IV-2 (Fig.1A) was used for enrichment of human exonic sequences with the NimbleGen SeqCap EZ Human Exome v2.0 Library (2.1 million DNA probes; Roche NimbleGen, Inc, Madison, WI). Sequencing was performed with 50 bp paired-end reads using Illumina (San Diego, CA) GAII (v2 Chemistry) to a mean depth of approximately 56x. All sequence reads were mapped to the reference human genome (UCSC hg 19) using the Illumina Pipeline software version 1.5 featuring a gapped aligner (ELAND v2). Variant identification was performed using GATK (McKenna et al., 2010). Amino acid changes were identified by comparison to the UCSC RefSeq database track. A local CCHMC realignment tool was used to minimize the errors in SNP calling due to indels. Exome data was initially screened for more than 300 genes known for cardiomyopathy or related phenotypes. Our filtering strategy removed previously reported variants in databases such as dbSNP (Sherry et al., 2001) and NHLBI Exome Sequencing Project (ESP) (http://evs.gs.washington.edu/EVS/), in addition to non-coding variants. Remaining variants were tested for segregation with disease in the family, and further subject to pathogenicity prediction programs including: Polyphen-2, SIFT/PROVEAN, MutationTaster, and HOPE (Adzhubei et al., 2010; Choi, Sims, Murphy, Miller, & Chan, 2012; Schwarz, Cooper, Schuelke, & Seelow, 2014; Venselaar, Te Beek, Kuipers, Hekkelman, & Vriend, 2010).

For Family 2, DNA samples were sent to the Advanced Genomics Laboratory at the Medical College of Wisconsin (MCW) for clinical ES of the parent and proband trio. In brief, after enriching for coding exons with solution based hybridization, an Illumina HiSeq

2500 was used for sequencing. Analysis of depth of coverage across exomes was performed with the GapMine software (MCW) with a minimum average depth of 85X. Sequencing variants were interpreted with the Carpe Novo software package (MCW). For this clinical pipeline, all identified variants were assessed for potential clinical significance. In addition to filtering variants based on quality and allele frequency, Carpe Novo uses multiple algorithms and databases to assess variants including bioinformatics predictions on protein function and structure (Polyphen-2 and SIFT), evolutionary conservation at the affected residues, changes to known splice site donors or acceptors, and presence or absence of the variant in aggregate databases such as dbSNP, HGMD, or OMIM (Stenson et al., 2003; https://omim.org/).

Variant screening and validation

Primers (Supp. Table S1) were designed covering exonic regions containing potential candidate variants (*FLNC, MYPN,* and *PKP2* in Family 1 and *FLNC* and *SYNE2* in Family 2). PCR products were sequenced on an ABI (Foster City, CA) 3730XL Genetic Analyzer using BigDye Terminator (ABI, Foster City, CA). Sequence analysis was performed via FinchTV (https://www.geospiza.com). All positive findings were confirmed in a separate experiment using the original genomic DNA sample as template for new amplification and bi-directional sequencing reactions. The *FLNC* p.Pro2298Leu and *FLNC* p.Tyr2563Cys variants (Refseq NM_001458.4) were determined to be pathogenic according to the American College of Medical Genetics (ACMG) 2015 guidelines for variant interpretation (Richards et al., 2015) based on data presented here (see Results). *FLNC* variants were submitted to ClinVar and have been assigned the following ClinVar accession numbers: SCV000787752 (p.Pro22298Leu) and SCV000787753 (p.Tyr2563Cys).

In silico protein homology modelling and viewing

SWISS-MODEL (Biasini et al. 2014) modeled the Ig domains 20-21 of FLNC to depict amino acid position 2298. The amino acid sequence of these domains was queried, and the template model most closely matching FLNC sequence was selected. This model was based on the known crystal structure of FLNA's Ig 20-21 domains (PDB 4P3W). A known crystal structure for FLNC Ig23 (PDB 2NQC) served as model to view amino acid position 2563. YASARA (Krieger & Vriend, 2014) was used to view both protein structures.

Cell culture, plasmid transfection, and immunocytochemistry

A human *FLNC* clone was purchased from Origene (Rockville, MD, catalog number RG212462) in a mammalian expression vector pCMV-AC-GFP. Mutagenesis was performed using primers designed (Supp. Table S2) for both the Q5 Site-Directed Mutagenesis Kit (New England Biolabs, Ipswich, MA) and the Infusion HD cloning kit (Clontech, Mountain View, CA). Validations of full length *FLNC* pCMV-AC-GFP plasmids with wild type and mutant transcripts were carried out using primers listed in Supp. Table S3. Both a standard calcium-phosphate method and Neon electroporation (Invitrogen, Waltham, MA) were used for transfections. For calcium-phosphate transfections, C2C12 cells (American Type Culture Collection, Manassas, VA; CRL-1772) were cultured with 2 mL Dulbecco's Modified Eagle Medium (DMEM) containing 10% fetal bovine serum (Hyclone, Pittsburgh, PA) and 1% penicillin-streptomyocyin (Gibco, Waltham, MA) in a 2 well ($4.0cm^2$) Lab-Tek chamber slide (Nunc, Rochester, NY) to reach 60% confluence on the day prior to transfection. To transfect, 5 µg of pCMV-AC-GFP *FLNC* wild type or mutant plasmids were combined with 8 µl of 2M $CaCl_2$. This mix was added dropwise to 62.5 µl 2X HEPES buffered saline. After 30 minutes of precipitation, the combined solution was added to the culture media and incubated overnight. After incubation, the transfection media was replaced with 2 mL fresh

media. For Neon electroporation, 100,000 C2C12 cells and 0.75µg of plasmid DNA were used in each transfection using electroporation conditions of 1,650 volts, 10 ms pulse width, and pulse number 3. Cells were plated into two well chamber slides with 2mL of the above described DMEM.

Forty-eight to 72 hours post transfection, cells were prepared for immunocytochemistry. All steps were carried out at room temperature. Cells were washed with phosphate buffered saline (PBS) 3 times for 15 minutes, fixed with 4% paraformaldehyde for 30 minutes followed by repeated PBS washes, and then permeabilized with 1% Triton-X100 (Fisher Scientific, Waltham, MA) for 30 minutes. Following permeabilization, blocking was carried out with 5% non-fat dried milk and 1% goat serum (Invitrogen, Waltham, MA) in 0.1% Tween-20 in PBS for 60 minutes. The following primary antibodies were incubated with cells for 3 hours: desmin (polyclonal rabbit α-mouse 1:200; Abcam, Cambridge, MA, ab8592) and FLNC (polyclonal goat α-mouse 1:500; Santa Cruz Biotechnology, Dallas, TX, sc-48496). Cells were washed with PBS and then incubated for 60 minutes in the following secondary antibodies, all at 1:100 dilutions: goat α-rabbit Alexa Fluor 568 (ThermoFisher, Waltham, MA); donkey α-goat Alexa Fluor 594 (ThermoFisher); and F-actin was detected with the Phalloidin-conjugated Alexa Fluor 594 (ThermoFisher). The slides were then rinsed in PBS buffer for 15 minutes, mounted with Vectashield containing DAPI for nuclei counterstain (Vector Laboratories, Burlingame, CA), and examined under a fluorescence (Nikon Eclipse E400, Melville, NY) or confocal microscope (Carl Zeiss Apotome, Thornwood, NY).

Pathology

Explanted heart tissue was fixed in 10% neutral buffered formalin for 24 hours at room temperature before embedding in paraffin (FFPE), sectioning, and staining with

hematoxylin and eosin (H&E) or trichrome. Additionally, a portion of the ventricle was fixed in 3% glutaraldehyde in cacodylate buffer, and sectioned to one cubic millimeter for processing and imaging by transmission electron microscopy.

Results

Phenotypic evaluation

Family 1 showed a typical autosomal dominant mode of inheritance (Fig. 1A), and all affected members presented with isolated RCM diagnosed at early ages. The family's race is African American. The proband was given a diagnosis of RCM at age 8, and upon echocardiogram was found to have an indexed left atrial volume of 72 ml/m^2, right atrial enlargement, and left ventricular diastolic dysfunction (Fig. 1B). Cardiac catheterization confirmed the diagnosis of RCM (Rindler, Hinton, Salomonis, & Ware, 2017). He underwent transplant at age 11. The patient's sister was followed by echocardiography due to the family history of RCM and first showed evidence of biatrial enlargement at age 4. She underwent cardiac catheterization and was given a diagnosis of RCM at age 5 and was listed for transplant which occurred at age 7. The paternal aunt was diagnosed with RCM at age 3 and the paternal half-sister was diagnosed under the age of 10. All of the affected individuals presented disease symptoms without evidence of myopathy or other extra-cardiac findings. Clinical genetic testing for 10 genes (*MYBPC3, MYH7, ACTC1, DES, MYL2, MYL3, TNNI3, TNNT2, TPM1,* and *EMD*) was performed as part of the clinical diagnostic evaluation and no sequence variants were reported by the clinical testing laboratory.

The proband in Family 2, is a 1 year old Caucasian female who presented with acute onset of unilateral weakness and was found to have a left sided thromboembolic middle cerebral artery stroke. Evaluation for etiology revealed classic phenotypic changes consistent with RCM including normal ventricular dimension and systolic function with massively

dilated atria (Fig. 2B). Of note, the child had an echocardiogram in the perinatal period that was normal aside from a small muscular ventral septal defect with restrictive left to right shunt. Due to elevated pulmonary vascular resistance, she was listed for heart transplant shortly after diagnosis and successfully transplanted months later. Family echocardiographic screening revealed her twin sister had similar phenotypic findings of RCM, while her brother, mother, and father were all unaffected (Fig. 2A). The twin sister progressed over months to require heart transplant listing and was successfully transplanted as well. Of note, each twin also presented with extra-cardiac phenotypes at the time of RCM diagnosis, including unspecified developmental delay, hypotonia, dysmorphic facial features, and clasped thumbs. Further, they each demonstrated kidney dysfunction of unclear etiology by three years of age, post heart transplant.

Pathology

Explanted heart tissue from the proband in Family 1 was processed for both histology and transmission electron microscopy (EM). H&E staining revealed some myocyte hypertrophy nuclear size changes, and occasionally central nuclei (Fig. 3A), whereas trichrome staining at lower magnification showed some differences in fiber sizes, and lacy interstitial fibrosis (Fig. 3B). EM of the explanted tissue showed essentially normal ultrastructure: there were no lipid or glycogen deposits. Relevant for FLNC-related myopathies, there were no inclusions or depositions observed. Mitochondrial organization and sarcomere structure (Fig. 3C-D) appeared normal and regular with no disarray, as is frequently seen in patients with *MYH7* or *MYBPC3* variants (Wessel et al., 2015; Witjas-Paalberends et al., 2013). The proband and twin sister from Family 2 also had explanted heart tissue processed for EM. Both proband (Fig. 3E) and sister (Fig. 3F) also demonstrate

regular sarcomeric structure, with no evidence of myofibril degeneration or signs of irregular mitochondria organization, aggregates, or depositions.

Exome analysis

After variant filtering, we identified 3 candidate variants in the proband in Family 1. These included variants in *MYPN* (p.Ser1282Arg)*, PKP2* (p.Val798Ile)*,* and *FLNC* (p.Pro2298Leu)*.* These sequence changes were tested in additional family members and only the *FLNC* missense variant p.Pro2298Leu (c.6893C>T; NM_001458.4) co-segregated with the RCM phenotype in the family, supporting a dominant mode of inheritance (Fig. 1C). The p.Pro2298Leu variant is located in exon 41 of *FLNC* and falls in the immunoglobulin-like (Ig) 20 (a.a. 2244-2306) domain of the protein.   This variant is not present in the Exome Aggregation Consortium (ExAC) (Lek et al., 2016). Additionally, the variant is located outside the region of homology transcribed *FLNC* shares with the identified *FLNC*-like pseudogene (Odgerel, van der Ven, Fürst, & Goldfarb, 2010).

Clinical ES of the trio and filtering strategies were used to identify potential disease causing variants in the proband of Family 2. Ultimately, three variants in two genes, *FLNC* and *SYNE2* (a gene associated with autosomal dominant Emery-Dreifuss muscular dystrophy), were filtered as being potentially clinically important. Each *SYNE2* variant (p.Val1688Ile and p.Lys4931Arg) was inherited from a healthy parent (Supp. Figure S1). Additionally, these variants were predicted to be benign by pathogenicity prediction, found in variant databases such as ExAC and dbSNP, and neither twin presented classical signs of Emery-Dreifuss by two years of age. The identified *FLNC* variant p.Tyr2563Cys (c.7688A>G; NM_001458.4) was present in both twins and absent in unaffected parents and sibling (Fig. 2C) indicating it was *de novo*. It was not found in ExAC or dbSNP, is located in Ig domain 23, and was confirmed to be in the functional *FLNC* gene and not its pseudogene.

In silico pathogenicity prediction

Both the autosomal dominant p.Pro2298Leu and *de novo* p.Tyr2563Cys variants in *FLNC* were unanimously predicted to be pathogenic using bioinformatic programs Polyphen-2, SIFT/PROVEAN, and Mutation Taster (Supp. Table S4). Further, the program HOPE (Venselaar, Te Beek, Kuipers, Hekkelman, & Vriend, 2010) was used to discover and analyze potential changes to protein structure resulting from each variant (Supp. Table S4). Proline at position 2298 of FLNC, as well as its respective triplet codon (CCC) in the gene, are evolutionary conserved across species suggesting an important role of this residue in protein function (Fig. 1D). Prolines are known to be very rigid and therefore induce a special backbone conformation which might be required at this position. All filamins consist of an N-terminus actin-binding domain followed by 24 antiparallel β-sheet repeats (called filamin or Ig-like domains), the 24th of which is responsible for filamin homo-dimerization at the C terminus (Stossel et al., 2001). These 24 Ig filamin repeats of the FLNC protein primarily form a secondary structure of beta strands, as seen in a model of Ig domains 20-21 (Fig. 4A) (Sjeklóca et al., 2007). The side chain of proline will typically disrupt β-strands due to its unique ring structure (Li, Goto, Williams, & Deber, 1996), and indeed proline 2298 falls in a loop between two such strands (Fig. 4B). The change to leucine at this position could disturb this special conformation and lead to protein aggregates. β-rich proteins like FLNC are prone to aggregation, and a leucine substitution could have a higher propensity to form hydrogen bonds between other nearby β-strands which could potentially disrupt protein folding and lead to aggregate formation (Hecht, 1994; Venselaar, Te Beek, Kuipers, Hekkelman, & Vriend, 2010).

Tyrosine at position 2563 is also evolutionarily conserved across species (Fig. 2D), and is located at the end of a β-strand (Fig. 4C-D). The mutant cysteine residue is less

hydrophobic and smaller than the wild type tyrosine, and due to its size is predicted to cause an empty space in the protein. The difference in hydrophobicity is also predicted to lead to a loss of hydrogen bonds at the core, which could disturb proper protein folding (Venselaar, Te Beek, Kuipers, Hekkelman, & Vriend, 2010). In addition to changes to hydrophobicity, the specific tyrosine to cysteine substitution may also be contributing to p.Tyr2563Cys protein aggregation (shown in results below). Substitution of tyrosine and cysteine at key resides of the human α-synuclein protein has been shown to cause accelerated protein aggregation *in vitro*, likely due to the increased ability for cysteine residues to cross-link and form stable dimers, which could be more prone to polymerization and aggregation (Zhou & Freed, 2004).

In vitro analysis of FLNC mutants

Previous studies of filaminopathies have shown evidence of mutant FLNC intracellular protein aggregation in both immuno-histological sections of patient muscle and in *in vitro* transfection of mutant *FLNC* constructs (Kley et al., 2007; Valdés-Mas et al., 2014; Vorgerd et al., 2005). These aggregates often contain additional Z-disk associated proteins such as desmin, a hallmark of myofibrillar myopathy. In order to determine whether the p.Pro2298Leu and p.Tyr2563Cys variants would also lead to intracellular protein aggregation, full-length wild type and mutant FLNC-GFP constructs were transiently expressed in C2C12 mouse myoblasts.

Cells expressing the wild type FLNC construct exhibited diffuse homogeneous expression of the protein (Fig. 5B and 5N), whereas the p.Pro2298Leu construct yielded aggregates (Fig. 5F and 5R), often near the nucleus. Additionally, the number of cells expressing p.Pro2298Leu mutant protein appeared considerably lower than those expressing the wild type FLNC construct. Cells expressing the mutant p.Tyr2563Cys construct also

demonstrated areas of FLNC aggregation (Fig. 5J and 5V), though these aggregates were punctate and varied in size from small to intermediate. Unlike the results seen with the p.Pro2298Leu construct, the diffuse FLNC expression was not lost in these cells; rather, the p.Tyr2563C aggregates appeared to be randomly distributed throughout otherwise normal protein expression. The pattern of aggregation observed for our p.Tyr2563Cys construct most closely mirrors what has been observed in cells transfected with *FLNC* variants causing distal myopathy (Duff et al., 2011). Additionally, unlike *FLNC* variants associated with myofibrillar myopathy, we did not observe the presence of desmin aggregation with mutant FLNC aggregates (Fig. 5S and 5W) or endogenous Flnc co-localizing to exogenous FLNC aggregates (Fig. 5G and 5K).

Given the importance of FLNC as an actin-binding protein, and *in vitro* data suggesting that *FLNC* variants may cause actin-aggregation (Kley et al., 2012), we transiently transfected p.Pro2298Leu and p.Tyr2563Cys constructs into C2C12 cells and stained for F-actin. As previously seen, the wild type FLNC construct showed diffuse cellular expression (Fig. 6A-D). The p.Pro2298Leu mutant again resulted in intracellular FLNC aggregates, but these cells also had actin aggregates which appear to co-localize with mutant protein (Fig. 6E-H). Taken together, these results suggest the p.Pro2298Leu variant results in an unstable, mutant protein which is prone to aggregation and may contribute to the overall weakening of myofibers as evidenced by actin aggregation. Cells transfected with the p.Tyr2563Cys construct also contained aggregates of both FLNC and F-actin (Fig. 6I-L), which again appeared more punctate, and varied in size. Overall, these data suggest the p.Tyr2563Cys is a potentially damaging variant, as it results in aggregates containing both FLNC and F-actin.

Discussion

In this study, we described two families with novel *FLNC* variants as disease causing for RCM: one, in a large family with autosomal dominant inheritance, and the other in a set of monozygotic, dichorionic/diamniotic twins with extra-cardiac features and a *de novo* variant. According to the 2015 ACMG variant interpretation guidelines, both variants can be classified as pathogenic. Our evidence to support pathogenicity for p.Pro2298Leu includes: damaging *in vitro* functional study (PS3); variant found in a mutation hot-spot of cardiomyopathy variants (PM1—see Table 1); variant absent from control databases (PM2); variant segregates with disease in family (PP1); computational evidence supports deleterious effect (PP3); and the patient and family have a disease consistent with a single genetic etiology (PP4). p.Tyr2563Cys is also pathogenic based on the following criteria listed above: PS3, PM1, PM2, PP3, and also a second strong level of evidence; the variant is *de novo* with maternity and paternity confirmed (PS2). Additionally we do not believe the twins' compound heterozygous *SYNE2* variants explain RCM, although it remains unclear whether they might contribute to some extra-cardiac features. In sum, we have discovered two new pathogenic *FLNC* variants causing an RCM phenotype.

FLNC is a Z-disk protein which binds to myozenin-1 and myotilin, and its expression is largely restricted to skeletal and cardiac muscles (Linnemann et al., 2010; van der Ven et al., 2006). In addition, FLNC interacts with the components of dystrophin-dystroglycan complex at the sarcolemma, thus acting as a scaffolding protein (Thompson et al., 2000). Altogether, Filamins interact with more than 90 cellular proteins with diverse functions including cell to cell and cell matrix connections, mechanoprotection, and various signaling networks (Feng & Walsh, 2004; Razinia, Mäkelä, Ylänne, & Calderwood, 2012). Recent data by Leber et al. (2016) show evidence of FLNC as a key early protein involved in myofibril repair for both skeletal and cardiac muscle cells. Their work suggests FLNC may be more of

a mobile signaling hub, rather than a largely structural and static protein (Leber et al., 2016). The early onset of RCM in the presented families suggests the importance of FLNC expression and its role in heart function.

FLNC variants are a recently recognized cause of phenotypically distinct cardiomyopathies including HCM, DCM, and RCM (Begay et al., 2016; Brodehl et al., 2016; Valdés-Mas et al., 2014). *FLNC*-related cardiomyopathies present a challenge in extrapolating genotype-phenotype correlations based on variant position (Table 1). Valdés-Mas et al., identified 8 HCM variants of which 2 are located in the actin binding domain, while the other 6 are distributed throughout the 24 filamin Ig domains. Interestingly, 5 of these 6 variants are located in C-terminal half of the protein and 4 are notably clustered in filamin repeats 18-22. A larger cohort of HCM patients sequenced by the same group identified additional candidate *FLNC* variants as potentially disease causing, most of which fell in the latter half of the protein (Gómez et al., 2017). Of interest, one likely pathogenic variant identified by Gómez et al. was at the same residue position (p.Pro2298Ser) as the variant reported here in family 1 (p.Pro2298Leu). The pattern of HCM variants falling in the C-terminal half of the protein is also seen with RCM variants: the two we report here fall in filamin repeats 20 and 23, a neighboring RCM variant to p.Pro2298Leu (p.Val2297Met) was recently reported by Tucker et al., 2017, and variants published by Brodehl et al. (2016) localize in repeats 14 and 19.

FLNC variants causing DCM have the most direct evidence of a genotype-phenotype relationship. Of the 8 previously reported DCM variants, 5 are splice site variants (Begay et al., 2016; Begay et al., 2018; Golbus et al., 2014), while 3 are nonsense variants resulting in an early protein truncation (Begay et al., 2018; Reinstein et al., 2016). Genetic screening of large DCM patient cohorts revealed an association with truncating *FLNC* variants (stop codons, frameshifts, and splice site variants), strongly suggesting an overlap between

mutation mechanisms and patient phenotype (Janin et al., 2017; Ortiz-Genga et al., 2016). Until recently, skeletal myopathy and cardiomyopathy-causing *FLNC* variants have been reported to cause isolated phenotypes in their respective tissues. Interestingly, however, a new publication has described disease-causing *FLNC* variants leading to both early-onset RCM and the skeletal muscle phenotypes congenital myopathy and clasped thumbs (Kiselev et al., 2018). The patients described here showed no evidence of myopathy on repeated exams although the twins did exhibit hypotonia. In light of the report by Kiselev et al. (2018), it is possible the p.Tyr2563Cys variant could be contributing to the twins' observed skeletal muscle phenotypes (hyoptonia and clasped thumbs), although this variant is not near the two variants Kiselev et al. found (p.Ala1183Leu and p.Ala1186Val). However, we do not believe the twins' other syndromic-like phenotypes, such as developmental delay and dysmorphic facial features, can likely be explained by a *FLNC* variant alone, and those hint at the possibility of a second underlying disorder. Additional functional studies will be necessary to determine the *FLNC* variant-specific effects resulting in isolated skeletal or heart muscle disease, or those which affect both tissues. In addition, mechanisms to explain the divergent cardiac phenotypes resulting from distinct *FLNC* variants remain to be elucidated.

Functional and structural analyses suggest that FLNC-mutants recruit FLNC-associated proteins to form aggregates, leading to destabilization of muscle tissue (Lowe et al., 2007; Luan, Hong, Zhang, Wang, & Yuan, 2010). Abnormal accumulations of FLNC deposits in patients' muscle tissues have been reported in a number of neuromuscular diseases (Bōnnemann et al., 2003; Sewry et al., 2002; Thompson et al., 2000). *In vitro* analyses for mutant FLNC p.Pro2298Leu revealed formation of perinuclear intracellular aggregates, while p.Tyr2563Cys expressing cells also formed point aggregates containing FLNC and F-actin, confirming the likely pathogenicity of these variants. Of note, similar experiments for HCM, DCM, and RCM *FLNC* mutants also resulted in aggregations of

mutant protein, many of which shared a similar pattern of aggregate expression around the nucleus (Brodehl et al. 2016, Reinstein et al., 2016; Valdés-Mas et al., 2014). The exact mechanism for this aggregate-based pathogenicity is unknown, but this could be an error in ubiquitination and lysosomal-dependent degradation of mutant FLNC as well as of other members of filamins.

Changes in filamin structure initiate the binding of the co-chaperone BAG3 as well as the ubiquitin ligase CHIP. CHIP ubiquitinates BAG3 and filamin leading to autophagy by p62 pathway (Arndt et al., 2010). Recent data suggest aggregates produced by the filamin C p.Trp2710X MFM variant in zebrafish were unable to be cleared properly by BAG3 and the chaperone assisted selective autophagy pathway (Ruparelia, Oorschot, Ramm, & Bryson-Richardson, 2016). Additionally, they noted the presence of BAG3 at these aggregates hindered alternative pathways that might have been able to remove them. Further studies of FLNC-aggregates produced by a wide range of variants are needed in order to elucidate the mechanisms by which these aggregates persist, and to develop potential methods to clear them.

In summary, we identified two novel *FLNC* missense variants causing a distinct RCM phenotype in two families, and further demonstrated these variants lead to protein localization defects *in vitro*. This study provides new variants and additional evidence for the wide spectrum of currently known *FLNC* variants, and bolsters support for the inclusion of *FLNC* in genetic testing of cardiomyopathy patients.

Acknowledgements

References

Ackerman, M. J., Priori, S. G., Willems, S., Berul, C., Brugada, R., Calkins, H., … Zipes, D. P. (2011). HRS/EHRA Expert Consensus Statement on the State of Genetic Testing for the Channelopathies and Cardiomyopathies. *Heart Rhythm*, *8*(8), 1308–1339. https://doi.org/10.1016/j.hrthm.2011.05.020

Adzhubei, I. A., Schmidt, S., Peshkin, L., Ramensky, V. E., Gerasimova, A., Bork, P., … Sunyaev, S. R. (2010). A method and server for predicting damaging missense mutations. *Nature Methods*, *7*(4), 248–249. https://doi.org/10.1038/nmeth0410-248

Arndt, V., Dick, N., Tawo, R., Dreiseidler, M., Wenzel, D., Hesse, M., … Höhfeld, J. (2010). Chaperone-Assisted Selective Autophagy Is Essential for Muscle Maintenance. *Current Biology*, *20*(2), 143–148. https://doi.org/10.1016/j.cub.2009.11.022

Avila-Smirnow, D., Gueneau, L., Batonnet-Pichon, S., Delort, F., Bécane, H.-M., Claeys, K., … Behin, A. (2016). Cardiac arrhythmia and late-onset muscle weakness caused by a myofibrillar myopathy with unusual histopathological features due to a novel missense mutation in FLNC. *Revue Neurologique*, *172*(10), 594–606. https://doi.org/10.1016/j.neurol.2016.07.017

Begay, R. L., Graw, S. L., Sinagra, G., Asimaki, A., Rowland, T. J., Slavov, D. B., … Taylor, M. R. G. (2018). Filamin C Truncation Mutations Are Associated With Arrhythmogenic Dilated Cardiomyopathy and Changes in the Cell–Cell Adhesion Structures. *JACC: Clinical Electrophysiology*. https://doi.org/10.1016/j.jacep.2017.12.003

Begay, R. L., Tharp, C. A., Martin, A., Graw, S. L., Sinagra, G., Miani, D., … Taylor, M. R. G.   (2016). FLNC Gene Splice Mutations Cause Dilated Cardiomyopathy. *JACC: Basic to   Translational Science*, *1*(5), 344–359. https://doi.org/10.1016/j.jacbts.2016.05.004

Biasini, M., Bienert, S., Waterhouse, A., Arnold, K., Studer, G., Schmidt, T., … Schwede, T. (2014). SWISS-MODEL: modelling protein tertiary and quaternary structure using evolutionary information. *Nucleic Acids Research*, *42*(W1), W252–W258. https://doi.org/10.1093/nar/gku340

Bönnemann, C. ., Thompson, T. ., van der Ven, P. F. ., Goebel, H. ., Warlo, I., Vollmers, B., … Schröder, R. (2003). Filamin C accumulation is a strong but nonspecific immunohistochemical marker of core formation in muscle. *Journal of the Neurological Sciences*, *206*(1), 71–78. https://doi.org/10.1016/S0022-510X(02)00341-6

Brodehl, A., Ferrier, R. A., Hamilton, S. J., Greenway, S. C., Brundler, M.-A., Yu, W., … Gerull, B. (2016). Mutations in FLNC are Associated with Familial Restrictive Cardiomyopathy. *Human Mutation*, *37*(3), 269–279. https://doi.org/10.1002/humu.22942

Choi, Y., Sims, G. E., Murphy, S., Miller, J. R., & Chan, A. P. (2012). Predicting the Functional Effect of Amino Acid Substitutions and Indels. *PLoS ONE*, *7*(10), e46688. https://doi.org/10.1371/journal.pone.0046688

Denfield, S. W., & Webber, S. A. (2010). Restrictive cardiomyopathy in childhood. *Heart Failure Clinics*, *6*(4), 445–452, viii. https://doi.org/10.1016/j.hfc.2010.05.005

Duff, R. M., Tay, V., Hackman, P., Ravenscroft, G., McLean, C., Kennedy, P., … Laing, N. G. (2011). Mutations in the N-terminal actin-binding domain of filamin C cause a distal

myopathy. *American Journal of Human Genetics*, *88*(6), 729–740. https://doi.org/10.1016/j.ajhg.2011.04.021

Feng, Y., & Walsh, C. A. (2004). The many faces of filamin: A versatile molecular scaffold for cell motility and signalling. *Nature Cell Biology*, *6*(11), 1034–1038. https://doi.org/10.1038/ncb1104-1034

FinchTV 1.4.0. Geospiza, Inc., (Seattle, WA), World Wide Web URL: http://www.geospiza.com

Gallego-Delgado, M., Delgado, J. F., Brossa-Loidi, V., Palomo, J., Marzoa-Rivas, R., Perez-Villa, F., … Garcia-Pavia, P. (2016). Idiopathic Restrictive Cardiomyopathy Is Primarily a Genetic Disease. *Journal of the American College of Cardiology*, *67*(25), 3021–3023. https://doi.org/10.1016/j.jacc.2016.04.024

Golbus, J. R., Puckelwartz, M. J., Dellefave-Castillo, L., Fahrenbach, J. P., Nelakuditi, V., Pesce, L. L., … McNally, E. M. (2014). Targeted analysis of whole genome sequence data to diagnose genetic cardiomyopathy. *Circulation. Cardiovascular Genetics*, *7*(6), 751–759. https://doi.org/10.1161/CIRCGENETICS.113.000578

Gómez, J., Lorca, R., Reguero, J. R., Morís, C., Martín, M., Tranche, S., … Coto, E. (2017). Screening of theFilamin CGene in a Large Cohort of Hypertrophic Cardiomyopathy Patients. *Circulation. Cardiovascular Genetics*, *10*(2). https://doi.org/10.1161/CIRCGENETICS.116.001584

Guergueltcheva, V., Peeters, K., Baets, J., Ceuterick-de Groote, C., Martin, J. J., Suls, A., … Jordanova, A. (2011). Distal myopathy with upper limb predominance caused by filamin C haploinsufficiency. *Neurology*, *77*(24), 2105–2114. https://doi.org/10.1212/WNL.0b013e31823dc51e

Harvey, P. A., & Leinwand, L. A. (2011). The cell biology of disease: Cellular mechanisms of cardiomyopathy. *The Journal of Cell Biology*, *194*(3), 355–365. https://doi.org/10.1083/jcb.201101100

Hecht, M. H. (1994). De novo design of beta-sheet proteins. *Proceedings of the National Academy of Sciences of the United States of America*, *91*(19), 8729–8730.

Janin, A., N'Guyen, K., Habib, G., Dauphin, C., Chanavat, V., Bouvagnet, P., … Millat, G. (2017). Truncating mutations on myofibrillar myopathies causing genes as prevalent molecular explanations on patients with dilated cardiomyopathy. *Clinical Genetics*, *92*(6), 616–623. https://doi.org/10.1111/cge.13043

Kaski, J. P., Biagini, E., Lorenzini, M., Rapezzi, C., & Elliott, P. (2012). Restrictive cardiomyopathy and hypertrophic cardiomyopathy overlap: the importance of the phenotype. *Cardiogenetics*, *2*(1). https://doi.org/10.4081/cardiogenetics.2012.e10

Kiselev, A., Vaz, R., Knyazeva, A., Khudiakov, A., Tarnovskaya, S., Liu, J., … Kostareva, A.   (2018). De novo mutations in FLNC leading to early-onset restrictive cardiomyopathy and congenital myopathy. *Human Mutation*. https://doi.org/10.1002/humu.23559

Kley, R. A., Hellenbroich, Y., van der Ven, P. F. M., Fürst, D. O., Huebner, A., Bruchertseifer, V., … Vorgerd, M. (2007). Clinical and morphological phenotype of the filamin myopathy: a study of 31 German patients. *Brain: A Journal of Neurology*, *130*(Pt 12), 3250–3264. https://doi.org/10.1093/brain/awm271

Kley, R. A., Serdaroglu-Oflazer, P., Leber, Y., Odgerel, Z., van der Ven, P. F. M., Olivé, M., … Fürst, D. O. (2012). Pathophysiology of protein aggregation and extended

phenotyping in filaminopathy. *Brain: A Journal of Neurology*, *135*(Pt 9), 2642–2660. https://doi.org/10.1093/brain/aws200

Kostareva, A., Kiselev, A., Gudkova, A., Frishman, G., Ruepp, A., Frishman, D., … Shlyakhto, E. (2016). Genetic Spectrum of Idiopathic Restrictive Cardiomyopathy Uncovered by Next-Generation Sequencing. *PLOS ONE*, *11*(9), e0163362. https://doi.org/10.1371/journal.pone.0163362

Krieger, E., & Vriend, G. (2014). YASARA View - molecular graphics for all devices - from smartphones to workstations. *Bioinformatics (Oxford, England)*, *30*(20), 2981–2982. https://doi.org/10.1093/bioinformatics/btu426

Leber, Y., Ruparelia, A. A., Kirfel, G., van der Ven, P. F. M., Hoffmann, B., Merkel, R., … Fürst, D. O. (2016). Filamin C is a highly dynamic protein associated with fast repair of myofibrillar microdamage. *Human Molecular Genetics*, *25*(13), 2776–2788. https://doi.org/10.1093/hmg/ddw135

Lek, M., Karczewski, K. J., Minikel, E. V., Samocha, K. E., Banks, E., … MacArthur, D. G. Exome Aggregation Consortium. (2016). Analysis of protein-coding genetic variation in 60,706 humans. *Nature*, *536*(7616), 285–291. https://doi.org/10.1038/nature19057

Li, S. C., Goto, N. K., Williams, K. A., & Deber, C. M. (1996). Alpha-helical, but not beta-sheet, propensity of proline is determined by peptide environment. *Proceedings of the National Academy of Sciences of the United States of America*, *93*(13), 6676–6681.

Linnemann, A., van der Ven, P. F. M., Vakeel, P., Albinus, B., Simonis, D., Bendas, G., … Fürst, D. O. (2010). The sarcomeric Z-disc component myopodin is a multiadapter protein that interacts with filamin and alpha-actinin. *European Journal of Cell Biology*, *89*(9), 681–692. https://doi.org/10.1016/j.ejcb.2010.04.004

Lowe, T., Kley, R. A., van der Ven, P. F. M., Himmel, M., Huebner, A., Vorgerd, M., & Furst, D. O. (2007). The pathomechanism of filaminopathy: altered biochemical properties explain the cellular phenotype of a protein aggregation myopathy. *Human Molecular Genetics*, *16*(11), 1351–1358. https://doi.org/10.1093/hmg/ddm085

Luan, X., Hong, D., Zhang, W., Wang, Z., & Yuan, Y. (2010). A novel heterozygous deletion–insertion mutation (2695–2712 del/GTTTGT ins) in exon 18 of the filamin C gene causes filaminopathy in a large Chinese family. *Neuromuscular Disorders*, *20*(6), 390–396. https://doi.org/10.1016/j.nmd.2010.03.009

McKenna, A., Hanna, M., Banks, E., Sivachenko, A., Cibulskis, K., Kernytsky, A., … DePristo, M. A. (2010). The Genome Analysis Toolkit: a MapReduce framework for analyzing next-generation DNA sequencing data. *Genome Research*, *20*(9), 1297–1303. https://doi.org/10.1101/gr.107524.110

Odgerel, Z., van der Ven, P. F. M., Fürst, D. O., & Goldfarb, L. G. (2010). DNA sequencing errors in molecular diagnostics of filamin myopathy. *Clinical Chemistry and Laboratory Medicine*, *48*(10), 1409–1414. https://doi.org/10.1515/CCLM.2010.272

Online Mendelian Inheritance in Man, OMIM®. McKusick-Nathans Institute of Genetic Medicine, Johns Hopkins University (Baltimore, MD), World Wide Web URL: https://omim.org/

Ortiz-Genga, M. F., Cuenca, S., Dal Ferro, M., Zorio, E., Salgado-Aranda, R., Climent, V., … Monserrat, L. (2016). Truncating FLNC Mutations Are Associated With High-Risk Dilated and Arrhythmogenic Cardiomyopathies. *Journal of the American College of Cardiology*, *68*(22), 2440–2451. https://doi.org/10.1016/j.jacc.2016.09.927

Razinia, Z., Mäkelä, T., Ylänne, J., & Calderwood, D. A. (2012). Filamins in Mechanosensing and Signaling. *Annual Review of Biophysics*, *41*(1), 227–246. https://doi.org/10.1146/annurev-biophys-050511-102252

Reinstein, E., Gutierrez-Fernandez, A., Tzur, S., Bormans, C., Marcu, S., Tayeb-Fligelman, E., … Lopez-Otın, C. (2016). Congenital dilated cardiomyopathy caused by biallelic mutations in Filamin C. *European Journal of Human Genetics*, *24*(12), 1792–1796. https://doi.org/10.1038/ejhg.2016.110

Richards, S., Aziz, N., Bale, S., Bick, D., Das, S., Gastier-Foster, J., … ACMG Laboratory Quality Assurance Committee. (2015). Standards and guidelines for the interpretation of sequence variants: a joint consensus recommendation of the American College of Medical Genetics and Genomics and the Association for Molecular Pathology. *Genetics in Medicine: Official Journal of the American College of Medical Genetics*, *17*(5), 405–424. https://doi.org/10.1038/gim.2015.30

Rindler, T. N., Hinton, R. B., Salomonis, N., & Ware, S. M. (2017). Molecular Characterization of Pediatric Restrictive Cardiomyopathy from Integrative Genomics. *Scientific Reports*, *7*, 39276. https://doi.org/10.1038/srep39276

Ruparelia, A. A., Oorschot, V., Ramm, G., & Bryson-Richardson, R. J. (2016). FLNC myofibrillar myopathy results from impaired autophagy and protein insufficiency. *Human Molecular Genetics*, *25*(11), 2131–2142. https://doi.org/10.1093/hmg/ddw080

Russo, L. M. (2005). Idiopathic restrictive cardiomyopathy in children. *Heart*, *91*(9), 1199–1202. https://doi.org/10.1136/hrt.2004.043869

Schwarz, J. M., Cooper, D. N., Schuelke, M., & Seelow, D. (2014). MutationTaster2: mutation prediction for the deep-sequencing age. *Nature Methods*, *11*(4), 361–362. https://doi.org/10.1038/nmeth.2890

Sewry, C., Müller, C., Davis, M., Dwyer, J. S. ., Dove, J., Evans, G., … Quinlivan, R. C. . (2002). The spectrum of pathology in central core disease. *Neuromuscular Disorders*, *12*(10), 930–938. https://doi.org/10.1016/S0960-8966(02)00135-9

Shatunov, A., Olivé, M., Odgerel, Z., Stadelmann-Nessler, C., Irlbacher, K., van Landeghem, F., … Goldfarb, L. G. (2008). In-frame deletion in the seventh immunoglobulin-like repeat of filamin C in a family with myofibrillar myopathy. *European Journal of Human Genetics*, *17*(5), 656–663. https://doi.org/10.1038/ejhg.2008.226

Sherry, S. T., Ward, M. H., Kholodov, M., Baker, J., Phan, L., Smigielski, E. M., & Sirotkin, K. (2001). dbSNP: the NCBI database of genetic variation. *Nucleic Acids Research*, *29*(1), 308–311.

Sjeklóca, L., Pudas, R., Sjöblom, B., Konarev, P., Carugo, O., Rybin, V., … Carugo, K. D. (2007). Crystal Structure of Human Filamin C Domain 23 and Small Angle Scattering Model for Filamin C 23–24 Dimer. *Journal of Molecular Biology*, *368*(4), 1011–1023. https://doi.org/10.1016/j.jmb.2007.02.018

Stenson, P. D., Ball, E. V., Mort, M., Phillips, A. D., Shiel, J. A., Thomas, N. S. T., … Cooper, D. N. (2003). Human Gene Mutation Database (HGMD): 2003 update. *Human Mutation*, *21*(6), 577–581. https://doi.org/10.1002/humu.10212

Stossel, T. P., Condeelis, J., Cooley, L., Hartwig, J. H., Noegel, A., Schleicher, M., & Shapiro, S. S. (2001). Filamins as integrators of cell mechanics and signalling. *Nature Reviews. Molecular Cell Biology*, *2*(2), 138–145. https://doi.org/10.1038/35052082

Tariq, M., & Ware, S. (2014). Importance of genetic evaluation and testing in pediatric cardiomyopathy. *World Journal of Cardiology*, *6*(11), 1156. https://doi.org/10.4330/wjc.v6.i11.1156

Tasca, G., Odgerel, Z., Monforte, M., Aurino, S., Clarke, N. F., Waddell, L. B., … Goldfarb, L. G. (2012). Novel FLNC mutation in a patient with myofibrillar myopathy in combination with late-onset cerebellar ataxia. *Muscle & Nerve*, *46*(2), 275–282. https://doi.org/10.1002/mus.23349

Thompson, T. G., Chan, Y. M., Hack, A. A., Brosius, M., Rajala, M., Lidov, H. G., … Kunkel, L. M. (2000). Filamin 2 (FLN2): A muscle-specific sarcoglycan interacting protein. *The Journal of Cell Biology*, *148*(1), 115–126.

Towbin, J. A. (2014). Inherited Cardiomyopathies. *Circulation Journal*, *78*(10), 2347–2356. https://doi.org/10.1253/circj.CJ-14-0893

Tucker, N. R., McLellan, M. A., Hu, D., Ye, J., Parsons, V. A., Mills, R. W., … Ellinor, P. T. (2017). Novel Mutation in *FLNC* (Filamin C) Causes Familial Restrictive Cardiomyopathy CLINICAL PERSPECTIVE. *Circulation: Cardiovascular Genetics*, *10*(6), e001780. https://doi.org/10.1161/CIRCGENETICS.117.001780

Valdés-Mas, R., Gutiérrez-Fernández, A., Gómez, J., Coto, E., Astudillo, A., Puente, D. A., … López-Otín, C. (2014). Mutations in filamin C cause a new form of familial hypertrophic cardiomyopathy. *Nature Communications*, *5*, 5326. https://doi.org/10.1038/ncomms6326

van der Ven, P. F. M., Ehler, E., Vakeel, P., Eulitz, S., Schenk, J. A., Milting, H., … Fürst, D. O. (2006). Unusual splicing events result in distinct Xin isoforms that associate

differentially with filamin c and Mena/VASP. *Experimental Cell Research*, *312*(11), 2154–2167. https://doi.org/10.1016/j.yexcr.2006.03.015

Vatta, M., & Towbin, J. A. (2011). Genetics of cardiomyopathies in children. *Cardiogenetics*, *1*(1). https://doi.org/10.4081/cardiogenetics.2011.e9

Venselaar, H., Te Beek, T. A. H., Kuipers, R. K. P., Hekkelman, M. L., & Vriend, G. (2010). Protein structure analysis of mutations causing inheritable diseases. An e-Science approach with life scientist friendly interfaces. *BMC Bioinformatics*, *11*, 548. https://doi.org/10.1186/1471-2105-11-548

Vorgerd, M., van der Ven, P. F. M., Bruchertseifer, V., Löwe, T., Kley, R. A., Schröder, R., … Huebner, A. (2005). A Mutation in the Dimerization Domain of Filamin C Causes a Novel Type of Autosomal Dominant Myofibrillar Myopathy. *The American Journal of Human Genetics*, *77*(2), 297–304. https://doi.org/10.1086/431959

Ware, S. M. (2015). Evaluation of genetic causes of cardiomyopathy in childhood. *Cardiology in the Young*, *25*(S2), 43–50. https://doi.org/10.1017/S1047951115000827

Ware, S. M. (2017). Genetics of paediatric cardiomyopathies. *Current Opinion in Pediatrics*, *29*(5), 534–540. https://doi.org/10.1097/MOP.0000000000000533

Webber, S. A., Lipshultz, S. E., Sleeper, L. A., Lu, M., Wilkinson, J. D., Addonizio, L. J., … on behalf of the Pediatric Cardiomyopathy Registry Investigators. (2012). Outcomes of Restrictive Cardiomyopathy in Childhood and the Influence of Phenotype: A Report From the Pediatric Cardiomyopathy Registry. *Circulation*, *126*(10), 1237–1244. https://doi.org/10.1161/CIRCULATIONAHA.112.104638

Wessels, M. W., Herkert, J. C., Frohn-Mulder, I. M., Dalinghaus, M., van den Wijngaard, A., de Krijger, R. R., … Dooijes, D. (2015). Compound heterozygous or homozygous

truncating MYBPC3 mutations cause lethal cardiomyopathy with features of noncompaction and septal defects. *European Journal of Human Genetics*, *23*(7), 922–928. https://doi.org/10.1038/ejhg.2014.211

Wilkinson, J. D., Westphal, J. A., Ross, S. W., Dauphin, D. D., & Lipshultz, S. E. (2015). The Value of National Institutes of Health (NIH) Registry-Based Research in Identifying Childhood Cardiac Disease Outcomes: The Pediatric Cardiomyopathy Registry Experience. In P. R. Barach, J. P. Jacobs, S. E. Lipshultz, & P. C. Laussen (Eds.), *Pediatric and Congenital Cardiac Care* (pp. 445–463). London: Springer London. Retrieved from http://link.springer.com/10.1007/978-1-4471-6587-3_34

Witjas-Paalberends, E. R., Piroddi, N., Stam, K., van Dijk, S. J., Oliviera, V. S., Ferrara, C., … van der Velden, J. (2013). Mutations in MYH7 reduce the force generating capacity of sarcomeres in human familial hypertrophic cardiomyopathy. *Cardiovascular Research*, *99*(3), 432–441. https://doi.org/10.1093/cvr/cvt119

Zhou, W., & Freed, C. R. (2004). Tyrosine-to-cysteine modification of human alpha-synuclein enhances protein aggregation and cellular toxicity. *The Journal of Biological Chemistry*, *279*(11), 10128–10135. https://doi.org/10.1074/jbc.M307563200

Figure Legends

Figure 1: Family 1 phenotypic and genetic evaluation. (**A**) Four-generation pedigree of Family 1 with autosomal dominant restrictive cardiomyopathy (RCM). DNA samples were available from individuals with a star. Proband IV-2 was analyzed by exome sequencing. (**B**) Echocardiogram image showing enlarged atria in the proband. (**C**) Sanger confirmation of *FLNC* variant (p.Pro2298Leu) in the affected proband and wild type allele in the unaffected mother (III-5). Arrows show the point of mutation (C>T). (**D**) Partial sequences of FLNC protein highlighting cross species conservation of proline residue at amino acid 2298.
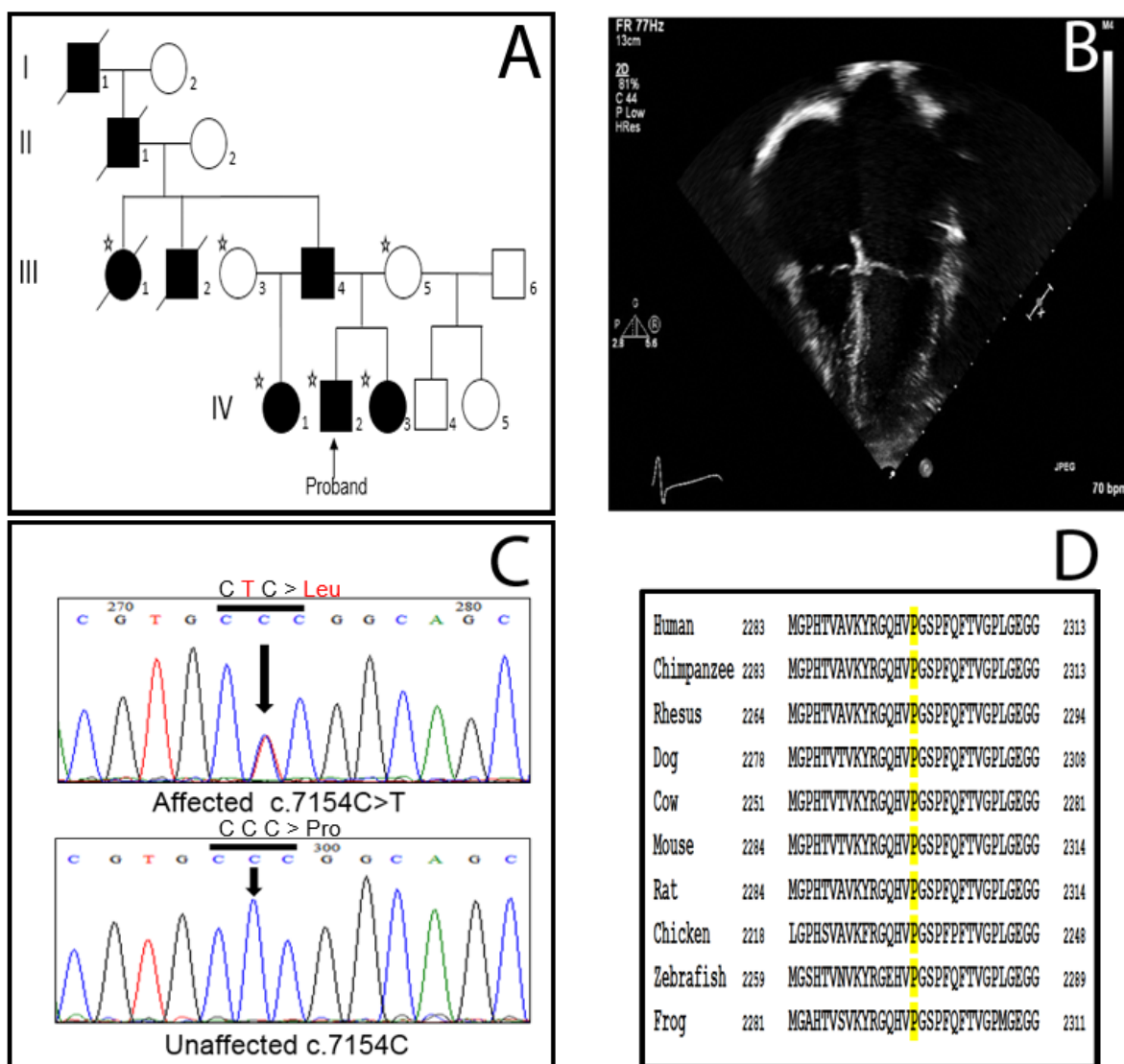
Figure 2: Family 2 phenotypic and genetic evaluation. (**A**) Four-generation pedigree of Family 2 with *de novo* RCM in twin sisters. DNA samples were available from individuals with a star sign. Proband IV-7 was analyzed by exome sequencing. (**B**) Echocardiogram image showing dilation of both atria in the proband. (**C**) Sanger confirmation of *FLNC* variant (p.Tyr2563Cys) in one twin and wild type allele in unaffected father and mother. Arrows show the point of mutation (A>G). (**D**) Partial sequences of FLNC protein highlighting cross species conservation of tyrosine residue at amino acid 2563.
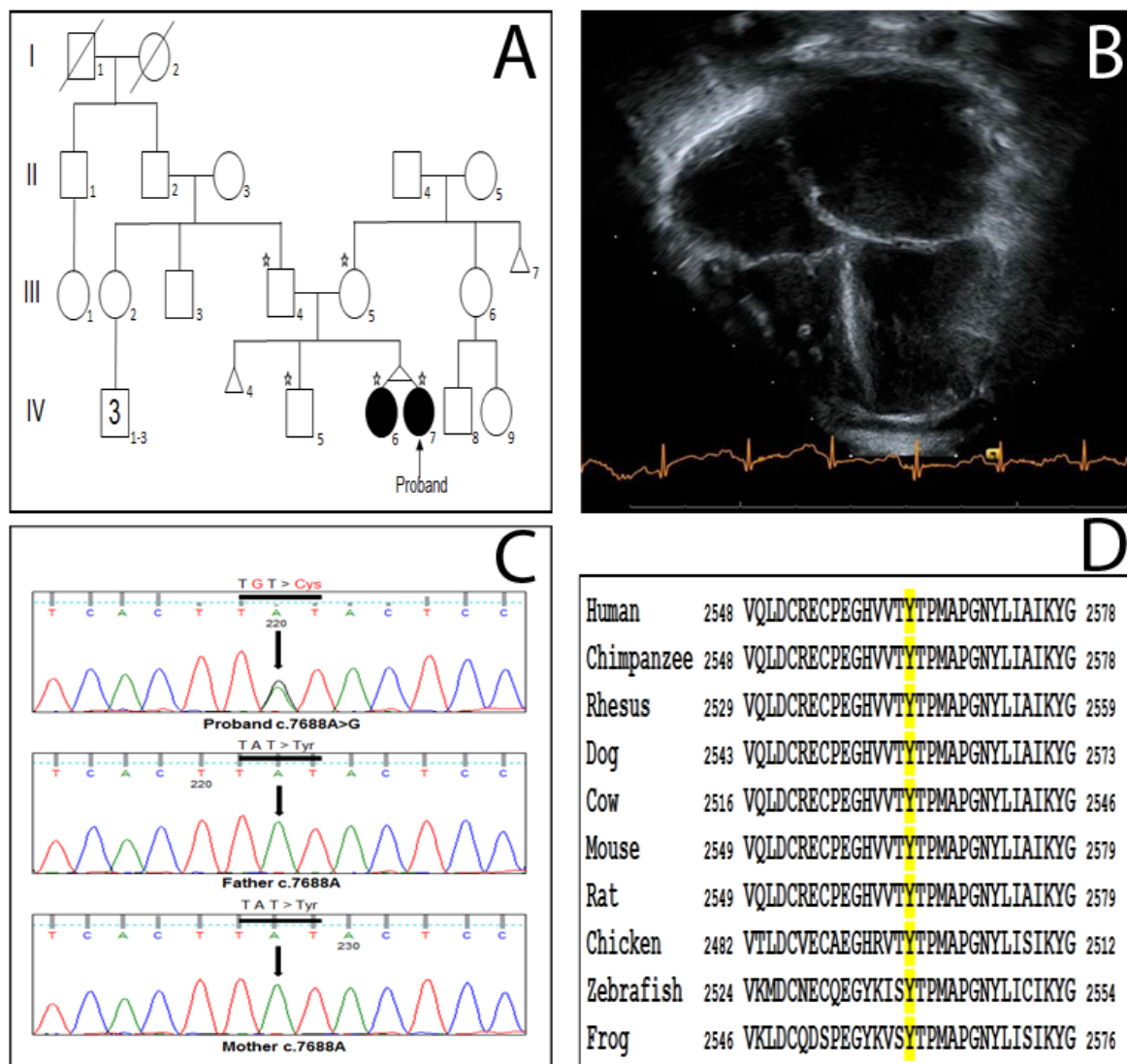
Figure 3: Pathological analysis of explanted heart tissue. (**A**) Hematoxylin and eosin (H&E) staining of ventricle from the proband of Family 1, 40X magnification. Black arrowheads denote examples of myocyte hypertrophy (**B**) Trichrome staining of ventricle from the proband of Family 1, 10X. Black arrows show examples of interstitial fibrosis. (**C**) Electron microscopy showing a magnified example of sarcomere structure in proband of Family 1, and (**D**) striated (z-lines) muscle cell structure with interspersed mitochondria. Panels **E** (proband) and **F** (twin sister) show representative EM images of sarcomeric structure from explanted heart tissues of Family 2.
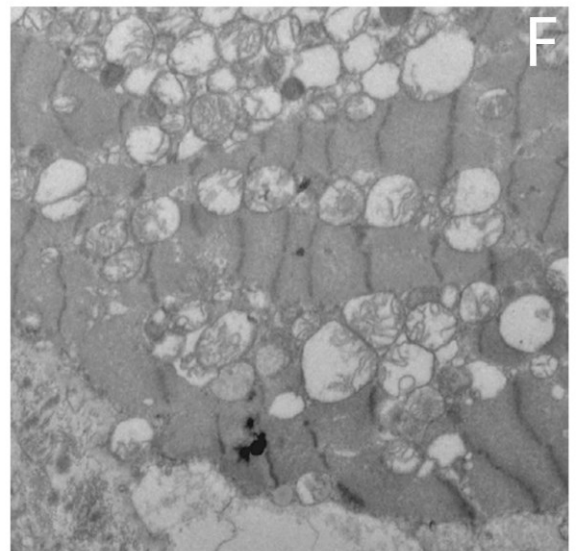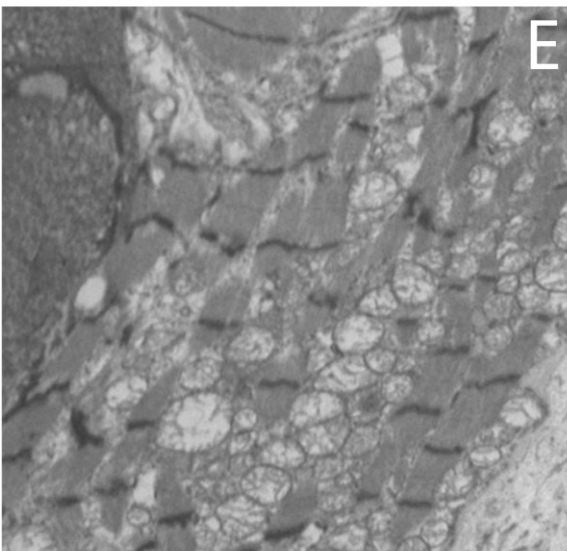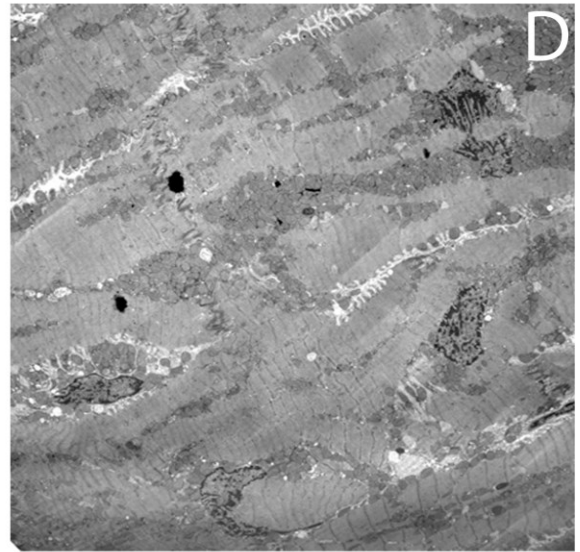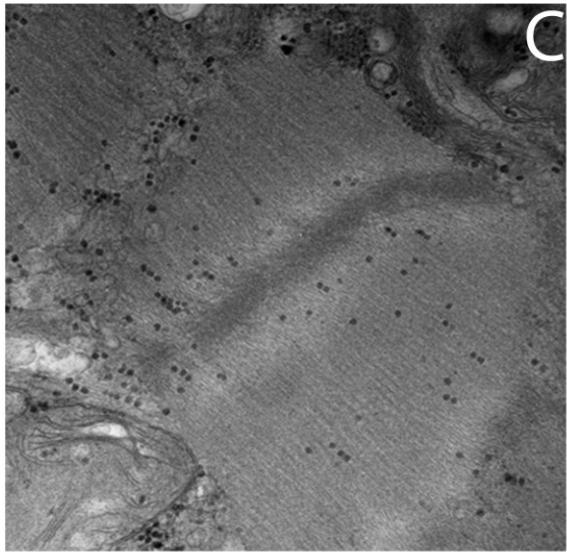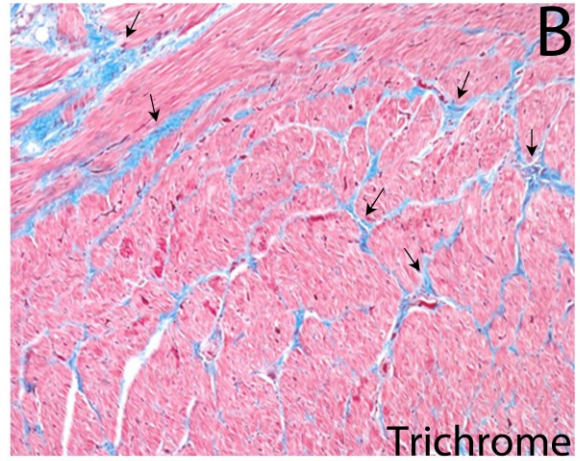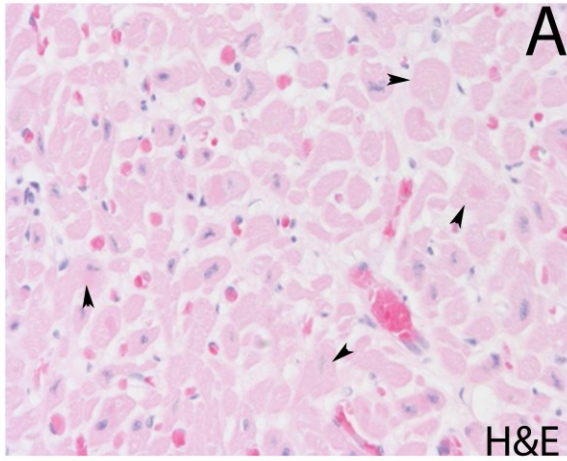
Figure 4: Protein modelling of FLNC variants. (**A**) An overview of FLNC protein domains Ig20-21 based on homology modeling using the known FLNA crystal structure of Ig20-21 (PDB 4P3W). P2298 falls in a "break" between two beta-strands, and is marked with an arrow. (**B**) A zoomed in view of the P2298 residue falling between beta-strands (colored yellow). Proline side chain is also depicted, which likely leads to disruption of strands. (**C**) An overview of FLNC protein domain Ig23 based on the available crystal structure (PDB 2NQC). Y2563 is located at the end of a beta strand, and is marked with an arrow. (**D**) A zoomed in view of the Y2563 residue (colored yellow); tyrosine side chain is also depicted.
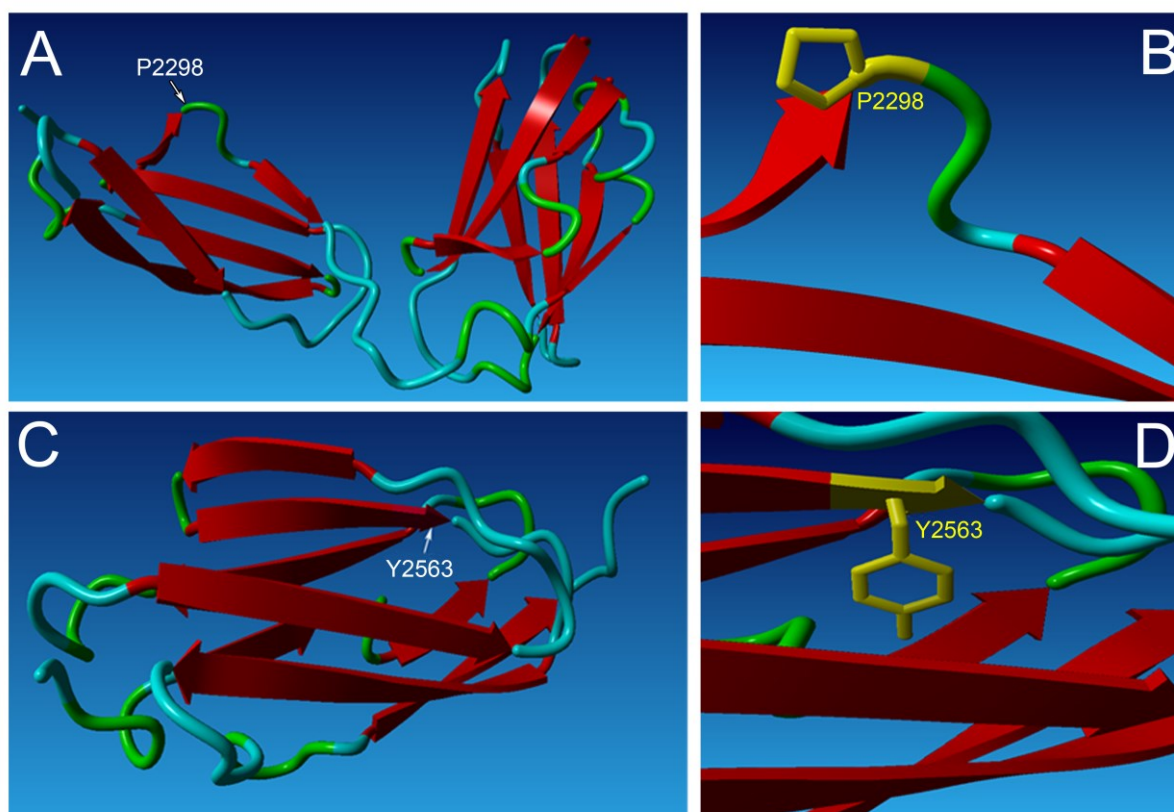
Figure 5: Expression of wild type and mutant FLNC in transiently transfected C2C12 cells. (**A-L**) Fluorescence microscopy images of C2C12 cells transfected with full-length wild type (**A-D**), p.Pro2298Leu (**E-H**), and p.Tyr2563Cys (**I-L**) FLNC constructs and counterstained for endogenous mouse Flnc (**C**, **G**, and **K**). (**M-X**) Fluorescence microscopy images of C2C12 cells transfected with wild-type (**M-P**), p.Pro2298Leu (**Q-T**), and p.Tyr2563Cys (**U-X**) FLNC constructs and counterstained for endogenous desmin (**O**, **S**, and **W**). All images have scale bars of 10μm, and 40X magnification. Arrows denote areas of mutant FLNC aggregation (panels **F**, **H, J**, **L, R**, **T, V**, and **X**).
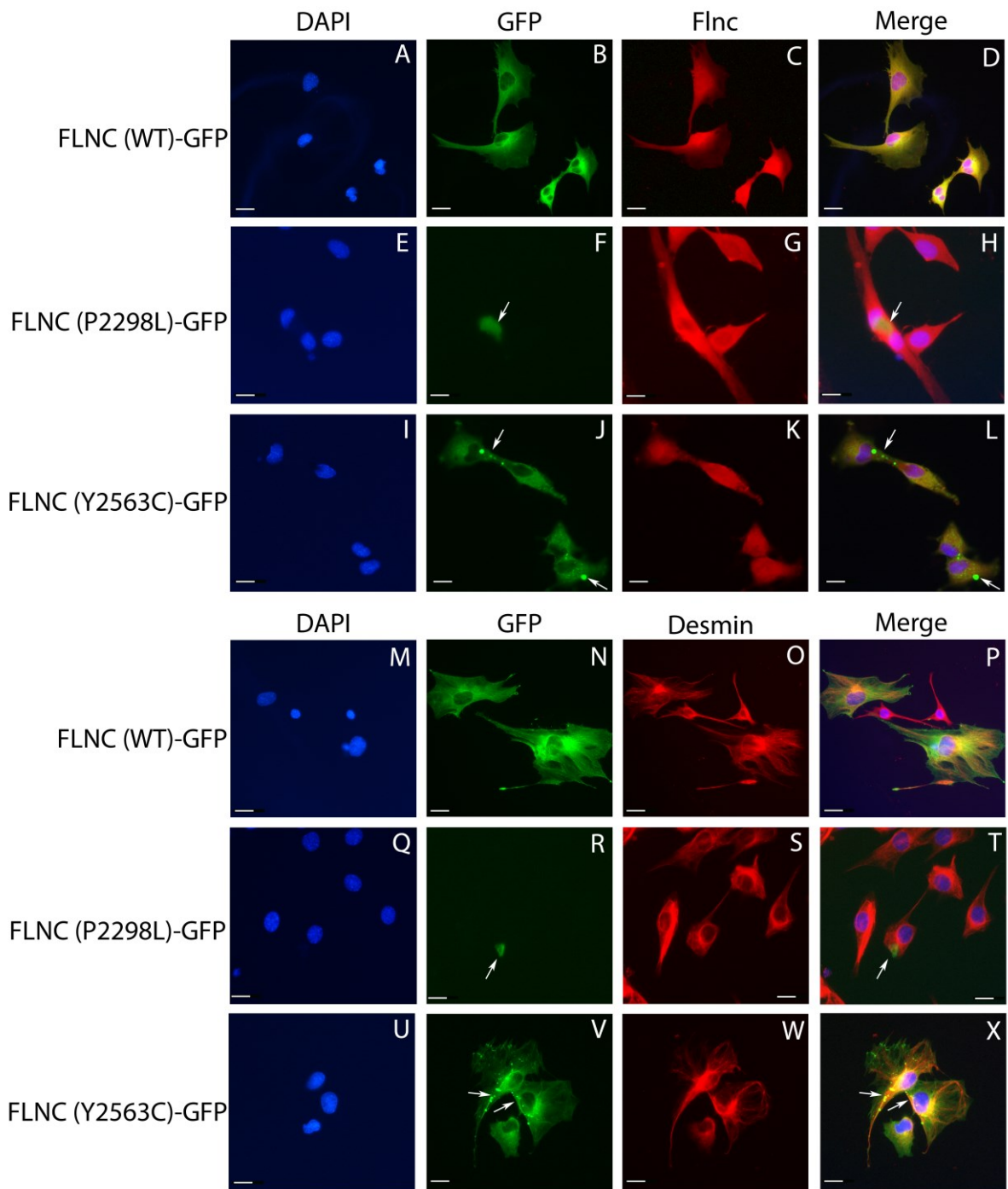
Figure 6: Actin aggregation in C2C12 cells transiently transfected with mutant FLNC. **(A-D)** Fluorescence microscopy images of C2C12 cells expressing the transfected wild type FLNC-construct. Scale bars 10μm, 40X magnification. **(E-H)** Confocal microscopy images of C2C12 cells expressing the mutant Pro2298Leu protein. Scale bars 10μm, 40X. **(I-L)** Cells expressing the mutant Tyr2563Cys protein. Scale bars 10μm, 40X. **(A, E, I)** Panels depict DAPI nuclear staining, (**B**, **F, J)** FLNC-GFP, **(C, G, K)** Phalloidin staining F-actin, **(D, H, L)** and a merged image of all three channels. Arrows denote areas of mutant FLNC and actin aggregation.
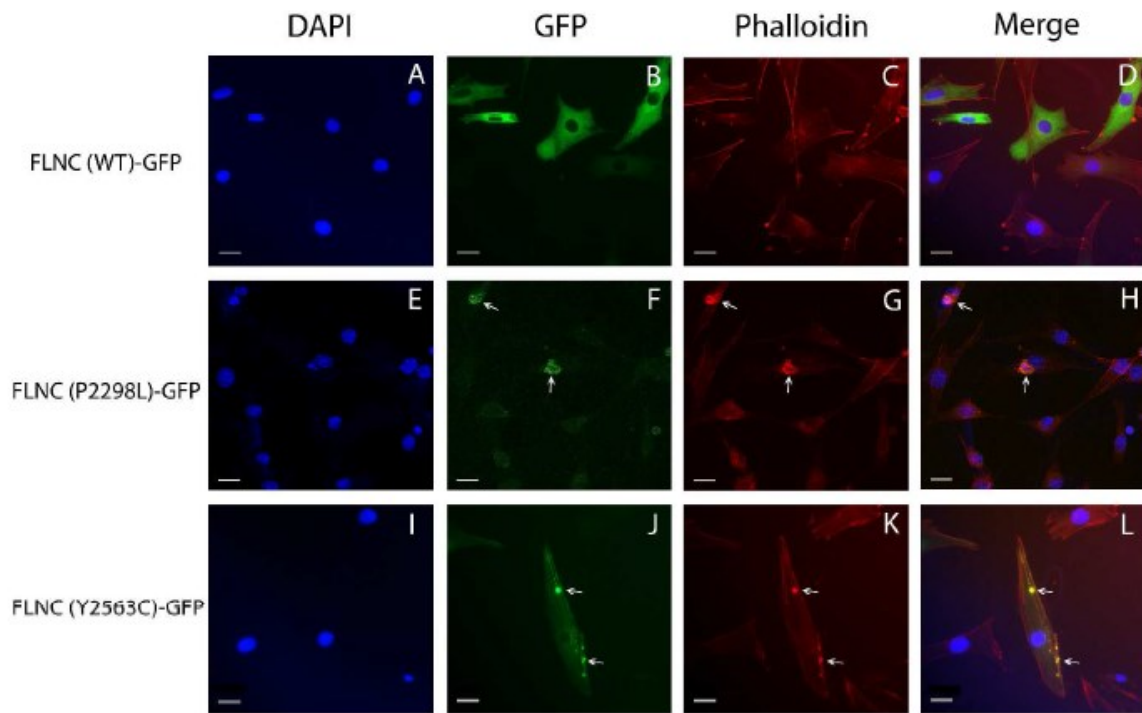
Table 1: Reported *FLNC* variants causing skeletal myopathy or cardiomyopathies. HCM = hypertrophic cardiomyopathy, DCM = dilated cardiomyopathy, RCM = restrictive cardiomyopathy, LV = left ventricle, AVC = Arrhythmogenic ventricular cardiomyopathy. Coding variants in reference to NM_001458.4 *FLNC* reference sequence.

Mutation	Domain with mutation	Exon	Mutation type	Phenotype	Disease onset	Number of families/cases associated	Cardiac involvement	Origin of Patient(s)	Reference
p.Phe106 Leu and p.Arg991Stop	Actin binding (1) and Filamin 8	1 and 20	Compound heterozygous	Dilated Cardiomyopathy	Less than 1 year	1 family with 2 patients	DCM	Ashkenazi	Reinstein et al. 2016
p.Glu108Stop	Actin binding (1)	1	Nonsense	Hypertrophic Cardiomyopathy	20-55 years	1 family with 2 patients	HCM	Spanish	Valdés-Mas et al. 2014
p.Val123Ala	Actin binding (1)	2	Missense	Hypertrophic Cardiomyopathy	33-44 years	1 family with 2 patients	HCM	Spanish	Valdés-Mas et al. 2014
p.Ala193Thr	Actin binding (2)	2	Missense	Distal Myopathy	30 years	1 family with 4 patients	2 patients with cardiomyopathy	Italian	Duff et al., 2011
p.Met251Thr	Actin binding (2)	4	Missense	Distal Myopathy	30 years	1 family with 9 patients	No	Australian	Duff et al., 2011
p.R269Stop	Filamin 1	4	Nonsense	Dilated Cardiomyopathy	20 years	1 family with 1 patient	DCM	N/A	Begay et al., 2018
p.Asn290Lys	Filamin 1	5	Missense	Hypertrophic Cardiomyopathy	50 years	1 family with 1 patient	HCM	Spanish	Valdés-Mas et al. 2014
p.Q707Stop	Filamin 5	13	Nonsense	Dilated Cardiomyopathy	33 years	1 Family with 1 patient	DCM	N/A	Begay et al., 2018
p.Lys899-Val904delinsValCys	Filamin 7	18	In-frame indel	Myofibrillar Myopathy	35-40 years	1 family with 10 patients	5 patients had Cardiac problems starting at 44, 52 and 59 years	Chinese	Luan et al., 2010
p.Val930_Thr933del	Filamin 7	18	In-frame deletion	Myofibrillar Myopathy	34-60 years	1 family with 2 patients	No	German	Shatunov et al., 2009
c.2930-1G>T	Filamin 8	Splice site before exon 19	Splice site	Dilated Cardiomyopathy	39 years	1 family with 1 patient	DCM	N/A	Begay et al., 2018

p.Ala1183Leu	Filamin 10	21	Missense	Restrictive Cardiomyopathy with Congenital Myopathy	RCM at 6 months, neuromuscular involvement at birth	1 family with 1 patient	RCM	N/A	Kiselev et al., 2018
p.Ala1186Val	Filamin 10	21	Missense	Restrictive Cardiomyopathy with Congenital Myopathy	RCM from 6 months to 15 years, neuromuscular involvement at birth or during first year	3 families with 3 patients	RCM	N/A	Kiselev et al., 2018
p.Tyr1216Asn	Filamin 10	21	Missense	Arrhythmia with Late-onset Myofibrillar Myopathy	NA	1 family with 9 patients	Cardiac arrhythmia	French	Avila-Smirnow et al., 2016
c.3791-1 G>C	Filamin 11	Splice site before exon 22	Novel splice-site acceptor, 53aa exclusion and frameshift	Dilated Cardiomyopathy	57 years	1 family with 2 patients	DCM	N/A	Golbus et al. 2014
c.3791-1G>A	Filamin 11	Splice site before exon 22	Novel splice-site acceptor, 53aa exclusion and frameshift	Dilated Cardiomyopathy	76 years	1 family with 1 patient	DCM	N/A	Begay et al., 2018
p.Ala1539Thr	Filamin 13	27	Missense	Hypertrophic Cardiomyopathy	20-82 years	1 family with 7 patients	HCM	Spanish	Valdés-Mas et al.2014
p.Ser1624Leu	Filamin 14	28	Missense	Restrictive Cardiomyopathy	2-40 years	1 family with 4 patients	RCM	Caucasian	Brodehl et al. 2016
p.Phe1720Leu fsX63	Filamin 15	30	Frameshift deletion	Distal Myopathy	20-57 years	3 families with 13 patients	1 patient has cardiomyopathy	Bulgarian	Guergueltcheva et al., 2011
c.5669-1delG	Filamin 17	Splice before	Splice site	Dilated Cardiomyopathy	46-53 years	1 family with 2 patients	DCM	USA	Begay et al. 2016 and 2018

Variant	Domain	Exon	Mutation	Disease	Age	Family/Patients	Type	Ethnicity	Reference
		exon 35							
p.Arg2133His	Filamin 18	39	Missense	Hypertrophic Cardiomyopathy	25-46 years	1 family with 2 patients	HCM	Spanish	Valdés-Mas et al. 2014
p.Gly2151Ser	Filamin 19	39	Missense	Hypertrophic Cardiomyopathy	20 years	1 family with 1 patient	HCM	Spanish	Valdés-Mas et al. 2014
p.Ile2160Phe	Filamin 19	39	Missense	Restrictive Cardiomyopathy	10-31 years	1 family with 6 patients	RCM	Caucasian	Brodehl et al. 2016
p.Val2297Met	Filamin 20	41	Missense	Restrictive Cardiomyopathy	14-51 years	1 family with 8 patients	RCM	N/A	Tucker et al. 2017
p.Pro2298Leu	**Filamin 20**	**41**	**Missense**	**Restrictive Cardiomyopathy**	**6-25 years**	**1 family with 6 patients**	**RCM**	**African American**	**This study**
p.His2315Asn	Filamin 21	41	Missense	Hypertrophic Cardiomyopathy	30-73 years	1 family with 3 patients	HCM	Spanish	Valdés-Mas et al. 2014
c.7251+1G>A	Filamin 22	Splice after exon 43	Predicted to remove splice donor for exon 43.	Dilated Cardiomyopathy	27-62 and 20-44 years	2 families, with 4 and 2 patients	DCM	Italian	Begay et al. 2016 and 2018
p.Thr2419Met	Filamin 22	44	Missense	Myofibrillar Myopathy with adult onset cerebellar ataxia	60 years	1 sporadic	Mild LV hypertrophy	Italian	Tasca et al., 2012
p.Ala2430Val	Filamin 22	44	Missense	Hypertrophic Cardiomyopathy	25-57 years	1 family with 3 patients	HCM	Spanish	Valdés-Mas et al. 2014
p.Tyr2563Cys	**Filamin 23**	**46**	**Missense**	**Restrictive Cardiomyopathy**	**Less than 1 year**	**1 family with 2 patients (twins)**	**RCM**	**Irish-German/ Polish-German**	**This study**
p.Trp2710Stop	Dimerization site	48	Nonsense	Myofibrillar Myopathy/ Limb-Girdle Muscular Dystrophy	37-57 years	1 family with 17 patients/1 family with 7 patients	No	German	Vorgerd et al., 2005
Multiple disease causing candidates	Protein spanning	Multiple	Truncating (stop, frameshift, indels)	Mostly dilated, or arrhythmogenic and few restrictive cardiomyopathies	Less than 1 to 71 years	28 affected probands and family members	DCM, AVC, RCM	Multiple European ethnicities	Ortiz-Genga et al., 2016
Multiple disease causing candidates	Protein spanning	Multiple	Missense, nonsense	Hypertrophic cardiomyopathy	21-64 years	16 affected probands and family members with likely pathogenic or VUS	HCM	Spanish	Gómez et al., 2017